Using molecular fragments to estimate electron-phonon coupling and possible superconductivity in covalent materials

Jonathan E. Moussa* and Marvin L. Cohen
Department of Physics, University of California at Berkeley, Berkeley, California 94720, USA
and Materials Sciences Division, Lawrence Berkeley National Laboratory, Berkeley, California 94720, USA
(Received 20 May 2008; published 1 August 2008)

We examine the electron-phonon coupling in a class of covalent materials by performing calculations on a set of molecular units from which they might be composed. By considering coupling to states at energies in the vicinity of the Fermi energy, we develop a picture of how couplings might be affected as these units are connected to form extended systems. Guided by this study of molecular fragments, we construct two examples of hypothetical covalent superconductors each with a transition temperature estimated to be ~380 K within Eliashberg theory. These hypothetical materials enter the regime of narrow-bandwidth metals where the superconducting state may be destabilized by one of several electronic instabilities and Eliashberg theory may no longer apply.

DOI: 10.1103/PhysRevB.78.064502 PACS number(s): 74.10.+v, 74.62.Bf, 74.70.Dd

I. INTRODUCTION

The class of covalent superconductors contains materials with the highest transition temperatures of all known conventional electron-phonon-mediated superconductors. The highest T_c values occur in MgB_2,[1] with a T_c of 40 K, and alkali-doped C_{60} compounds,[2] with T_c up to 38 K under pressure[3] and 33 K at ambient pressure. Also of note is boron-doped diamond, which has achieved a T_c of 11 K despite having a very low carrier density.[4] Specific theoretical proposals have been made for hypothetical higher-T_c materials by doping covalently bonded materials, such as boron icosahedra,[5] carbon clathrates,[6] and BC_3 graphite.[7] Theory also suggests that the T_c of boron-doped diamond may also rise with further increases in boron concentration.[8] Some relevant observations which have been made about electron-phonon coupling in molecules suggest that there is a correlation between large electronegativity and large electron-phonon coupling strength[9] and that coupling is inversely proportional to the size of a molecule.[10] There is however a lack of any general estimates for the strength of electron-phonon coupling in covalent materials. If available, these may at least serve to set reasonable expectations for future discoveries and at best may provide plausible bounds on achievable values of T_c.

For the desirable goal of strongly coupling superconductors, it was shown by Allen and Dynes[11] that T_c is proportional to the quantity $\sqrt{\lambda\langle\omega^2\rangle}$, which is a measure of electron-phonon coupling strength that is insensitive to details of the phonon spectrum. An atom-centric description of $\lambda\langle\omega^2\rangle$ was given by Hopfield,[12] where coupling strength is limited by an angular-momentum selection rule. Later work by Lam and Cohen[13] successfully fits $\lambda\langle\omega^2\rangle$ of all the elemental superconductors to a simple model dependent only on the densities of atoms and valence electrons. These models cannot be applied to covalent materials because of a lack of simple descriptions for Bloch states comprised of a superposition of covalent bonding states or the local-field effects that screen the potential induced by atomic displacements. However, both the electronic states and screening in covalent materials are readily captured by modern density-functional theory (DFT) calculation, which is the basis for calculations of electron-phonon coupling in specific material proposals.[14] Using the principle of nearsightedness of electronic properties,[15] we can build up a model of electron-phonon coupling in covalent materials by partitioning materials into common molecular fragments and performing careful DFT calculations independently on individual fragments. This is very much in the spirit of organic chemistry, where structure is largely determined by local bonding and shell-filling rules. The vast combinatorial complexity of possible structures built to satisfy these chemical rules can be avoided if the properties of the connected materials are similar enough to the molecular fragments from which they are built.

The variety and tunability that may be possible in covalent materials enables the adjustment of properties relevant to superconductivity and an engineering of high transition temperatures. The first ingredient that enables this engineering is independent control over the electronic density of states at the Fermi level and electron-phonon coupling strength. This is achieved when the electron-phonon coupling is associated with intramolecular-fragment vibrations and bonds, while the density of states is determined by inter-fragment hopping and bonds. For example, in the C_{60} compounds the electron-phonon coupling is dominated by the breathing modes of the C_{60} molecule and the density of states is inversely proportional to the overlap of π orbitals between neighboring molecules.[2] The second ingredient is the ability to electronically dope a material over a wide range of concentrations. This might be accomplished by controlled intercalation of interstitial dopant atoms in an open framework, as is the case with the alkali atoms in the C_{60} compounds, or deintercalation in the case of $Li_{1-x}BC$.[16] Materials satisfying these design criteria might arise from crystallization, chemical vapor deposition, or polymerization of some combination of precursor molecules. The experimental syntheses of open, covalently bonded metal-organic frameworks[17] and planar BC_3 (Ref. 18) are examples that demonstrate the possibility of synthesizing ordered covalent materials using these techniques.

Studying the electron-phonon coupling in molecular fragments cannot bound the attainable T_c because the electronic density of states is only limited by instabilities that are not properties of the fragments. The Eliashberg theory of electron-phonon superconductivity[19] requires Migdal's theorem[20] to be satisfied in order to be valid. Narrow bands at the Fermi level because of very weak coupling between molecular fragments can violate the criterion that the electronic bandwidth is much larger than the phonon frequencies mediating superconductivity. Other instabilities associated with narrow bands, such as magnetism and the Mott transition, may compete with superconductivity and further violate the standard Eliashberg theory treatment of Coulomb interactions as a renormalized Coulomb pseudopotential.[21] There are additional instabilities directly associated with electron-phonon coupling, such as static structural instability that opens an insulating electronic gap or dynamical gap opening arising from polaronic behavior.[22] Even in the C_{60} compounds, some of these effects are already pronounced and treatment of correlation beyond mean-field theory is required to understand the deviation of T_c from the Eliashberg theory result.[23] Recent experiments on C_{60} have clearly driven the system across a superconducting-insulator transition as a function of volume per C_{60},[3] which tunes the electronic bandwidth. Placing a bound on T_c will require a careful theoretical consideration of all instabilities of the superconducting state and is beyond the scope of this paper.

The goal of this paper is to present empirical observations on electron-phonon coupling trends based on calculations of a variety of molecular fragments that are representative of the bonds that one would expect to find in a covalent material. Guided by these observations, we construct two examples of hypothetical superconductors from molecular fragments, both of which are calculated to have large T_c values within Eliashberg theory. These hypothetical superconductors may serve as specific synthesis targets for experimentalists and as specific cases in which to study the stability of the superconducting state for theorists. All DFT calculations performed in this paper utilized the VASP computer code[24] with projector augmented wave (PAW) pseudopotentials and the Perdew-Burke-Ernzerhof (PBE) exchange-correlation functional.

II. TRENDS IN MOLECULAR FRAGMENTS

As a metric for electron-phonon coupling strength in molecular fragments, we use the quantity $\sqrt{\lambda\langle\omega^2\rangle}$. This quantity bounds T_c within Eliashberg theory,[11]

$$T_c \leq 0.18\sqrt{\lambda\langle\omega^2\rangle}, \tag{1}$$

and this bound is approached as $\lambda \to \infty$. In terms of the Γ-point approximation to the Eliashberg spectral function that was successfully used to describe superconductivity in heavily boron-doped diamond,[8] the metric takes the form

$$\lambda\langle\omega^2\rangle = \sum_{i,j} \frac{1}{M_j} \left| \frac{d\epsilon_i}{d\mathbf{R}_j} \right|^2 \delta(\epsilon_F - \epsilon_i), \tag{2}$$

where i is summed over electronic states in the system not including spin and j is summed over atoms. This expression measures coupling to electronic states at the Fermi energy ϵ_F, but it can easily be evaluated on other energy surfaces as it takes the form of a projected density of states. Calculations for energies other than ϵ_F are rigid-band approximations to doping scenarios. This allows for the comparison of electron-phonon coupling strengths to shallow states that can be realistically accessed by physical modifications with states too deep in energy to be moved to the Fermi surface.

For Eq. (2) to have a finite value for molecular clusters, the delta functions are replaced by normalized Gaussians, which represent an artificial dispersion of the molecular-orbital energies. This smearing of the delta functions is necessary even for extended systems to converge the expression given only a finite sampling of electronic states in the Brillouin zone. A smearing of 0.4 eV is chosen as has previously been used for extended systems.[8] By using the same values of smearing, we can make comparisons between different molecular fragment calculations and further compare these to bulk material calculations. Most fragment calculations are performed in a 1 nm^3 cubic unit cell using only the Γ point for electronic properties and are structurally relaxed. A 1.2^3 nm^3 cell is used for a few of the larger fragments—the C_{60} fullerene, C_8H_{18} linear alkane, and $C_{41}H_{60}$ diamondoid. The value of ϵ_F for insulating systems is set to the average value of the mean-field potential. As degeneracies of energy levels are not clear from plotting $\lambda\langle\omega^2\rangle$ as a function of energy, the energy levels and their degeneracies are also plotted in the figures to follow. Some unoccupied states are part of the continuum of free-electron-like unbound states and their specific energies and wave functions are just artifacts of the Γ-point sampling of the unit cell.

The electron-phonon coupling metric used in this paper differs from another popular metric used for molecules,[10]

$$V_{\mathrm{ep}} = \frac{1}{\nu^2} \sum_{i,j} \frac{1}{\omega_j^2} \left| \sum_k \frac{[\xi_j]_k}{\sqrt{M_k}} \frac{d\epsilon_i}{d\mathbf{R}_k} \right|^2, \tag{3}$$

where i is summed over the ν degenerate electronic states at ϵ_F, j is summed over phonon modes, k is summed over atoms, and ω_j and ξ_j are phonon frequencies and displacement vectors. This other metric is meant for estimating $\lambda = N_\uparrow(\epsilon_F) V_{\mathrm{ep}}$ given the density of states per spin at the Fermi level $N_\uparrow(\epsilon_F)$. This is useful for studying superconductivity in the weak- and intermediate-coupling regimes, but it contains phonon details that are irrelevant in the strong-coupling regime. In addition, this metric averages the electron-phonon coupling contributions of degenerate energy levels rather than summing them. Degeneracies in the energy levels of molecules can lead to a degenerate manifold of bands when the molecules are ordered in a crystal provided that there are no strong crystal-field effects. Such degenerate bands may lead to larger values of $N_\uparrow(\epsilon_F)$ for comparable bandwidths with respect to an isolated band. The usefulness of electronic degeneracies should be included in a metric for electron-phonon coupling, as is the case in Eq. (2). For a carefully designed material, degeneracies in molecular fragment building blocks may lead to density-of-states peaks in the final material. Assuming that the electronic states are uniformly spread over the N atoms of a molecule and that the potential

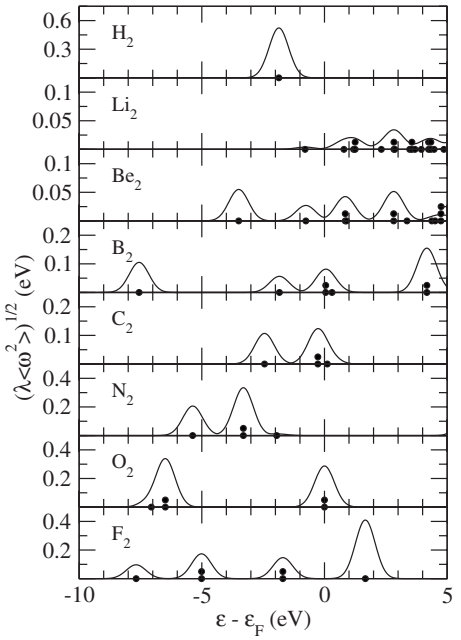

FIG. 1. Electron-phonon coupling strength in symmetric dimers. Black circles denote energy levels and their stacking denotes degeneracy of levels.

change from perturbing an atom is well localized to the vicinity of the atom, then Eq. (3) scales as N^{-1}. With the inclusion of electronic degeneracies in Eq. (2), the metric's scaling becomes independent of N since an extensive contribution from the sum over electrons cancels the N^{-1} scaling.

The effects missing in Eq. (2) when comparing the properties of molecular fragments and extended materials are all associated with breakdowns of the nearsightedness of electronic properties in metallic systems. The joining of molecular fragments to form an extended system will spread molecular orbitals into bands and cause hybridization between orbitals if the hopping energy is large enough. Crystal-field effects can further break electronic degeneracies in the molecular fragments and redistribute electron-phonon coupling strength to different energies. Metallic screening present only in the extended metallic system should cause an overall reduction in electron-phonon coupling strength compared to fragment calculations, especially for large values of $N_{\uparrow}(\epsilon_F)$.

A. Symmetric dimers

Since there is no electron-phonon coupling for an isolated atom, the simplest fragment to study is a dimer. Since light masses are favorable for increasing Eq. (2), we consider first- and second-row elements. This should reflect trends for other rows of the Periodic Table. In order to maximize covalency, we minimize ionicity by choosing dimers of identical atoms. The values of $\lambda\langle\omega^2\rangle$ as a function of electronic energy are plotted in Fig. 1. There is a clear trend in coupling strength that follows electronegativity and dimer stability. The Li_2, Be_2, and B_2 dimers are not chemically stable in the solid state as reflected in their small or nonexistent highest occupied molecular orbital (HOMO)–lowest unoccupied molecular orbital (LUMO) gaps. The H_2, N_2, O_2, and F_2 are all gapped and stable, while C_2 is a stable ion with two additional electrons. The electronic gap in O_2 is a singlet-triplet gap that is not captured in these calculations. In going from left to right in the Periodic Table, there is a trend of increasing electron affinity. Atoms with larger electron affinity draw the electronic states closer where they overlap more strongly with the potentials resulting from atomic perturbations. This effect serves to enhance the electron-phonon coupling strength. Ignoring mass factors in Eq. (2), the largest displayed coupling in a symmetric dimer comes from the LUMO state of F_2. The strongest overall coupling comes from H_2 because of its smaller mass factor. Related to trends in electron affinity, the correlation between electronegativity and electron-phonon coupling has been previously noted.[9]

Empirically, the dimer stability is anticorrelated with the ability for these elements to form a metallic state. This leads to an unfortunate anticorrelation between strong electron-phonon coupling and a metallic state, the coincidence of which is required for high-temperature superconductivity. The superconducting potential of H_2 was realized early on, and it was suggested that its metallization could be driven by extreme pressures that dissociate the molecule.[25] Of the stable dimers studied here, only O_2 has yet been forced by pressure into a superconducting state,[26] with a T_c of 0.6 K. To date, more success has been achieved by the application of pressure on a preformed metallic state, such as lithium[27] and calcium,[28] where pressure preserves metallicity while pushing the atoms closer together to increase covalency and electron-phonon coupling strength, reaching T_c values of 20 and 25 K.

B. *X*-H bonds

While superconductivity in pure hydrogen has yet to be achieved, there is a growing interest in high-pressure metallization of hydrogen-rich materials[29] that has led to an experimental realization of superconducting SiH_4 with a T_c of 17 K.[30] In Fig. 2, we compare the electron-phonon coupling strength in SiH_4 with molecules consisting of second-row elements bonded to one or more hydrogen atoms. There is again a trend of increasing electron-phonon coupling with increasing electronegativity. However, for molecules with lone pairs, such as NH_3 and H_2O, the lone pair electrons dominate the HOMO state and reduce electron-phonon coupling near ϵ_F. In contrast, the HOMO state of the tetrahedral NH_4^+ unit has the largest electron-phonon coupling among this set of molecules.

Study of the SiH_4 molecule under pressure was theoretically proposed based on evidence that it may be easier to metallize under pressure than other XH_n molecules.[31] If one uses the DFT HOMO-LUMO gap as an indication of susceptibility to high-pressure metallization, BH_4^- may be a good candidate for future studies. Because it is an anion, the choice of cation is an additional material degree of freedom when studying compounds containing BH_4^-. While NH_4^+ has the largest electron-phonon coupling, it also has the largest HOMO-LUMO gap of 13.8 eV and may thus be the hardest molecule in this set to metallize. One caveat of comparisons to SiH_4 is that within the high-pressure superconducting

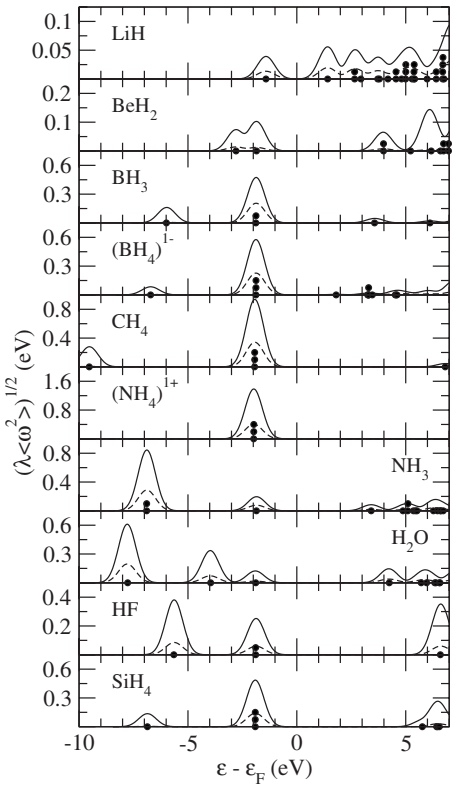

FIG. 2. Electron-phonon coupling strength in XH_n molecules. Dashed curves omit the contribution from H atoms. Black circles denote energy levels and their stacking denotes degeneracy of levels.

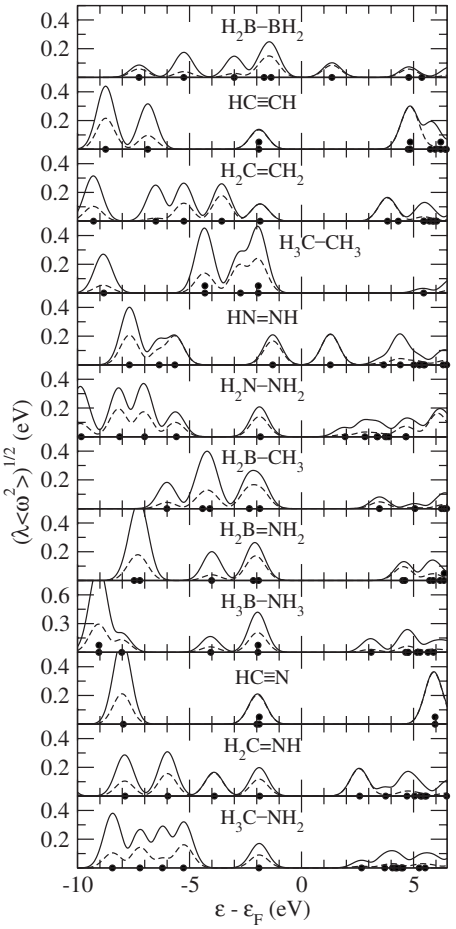

FIG. 3. Electron-phonon coupling strength in H-terminated molecules with a single B-C-N bond. Dashed curves omit the contribution from H atoms. Black circles denote energy levels and their stacking denotes degeneracy of levels.

structure the SiH_4 molecules have been decomposed. The bond energy might be more relevant than the HOMO-LUMO gap in determining whether pressure will metallize a XH_n molecule. The more strongly covalent second-row elements have larger bond energies than silicon.

C. B-C-N covalent bonds

Commonly studied classes of covalent materials are those containing boron, carbon, and nitrogen. Except, for instances, of aromatic carbon rings and boron clusters, these materials can be considered to be composed of distinct single, double, or triple bonds between atoms. From this combination of bond order and atoms, we construct a set of hydrogen-terminated dimers XYH_n. Electron-phonon coupling strengths of these molecules are plotted in Fig. 3. Of these bonds, the C-C and B-N single bonds lead to the largest electron-phonon coupling to the HOMO state. The B-B single bond and N-N double bond have the smallest HOMO-LUMO gaps. In the case of boron, this leads to XB_2 materials, most notably MgB_2, with significant electron doping of the B-B single bond to form a superconducting, graphitelike plane. The strong electron-phonon coupling in the N-N double bond may be similarly conducive to doping through careful material design and synthesis. The HOMO states of these molecules have much smaller electron-phonon contributions from the hydrogen atoms compared to the XH_n molecules in Fig. 2. The cause of this trend is that the *X*-*Y* bonding states are higher in energy than the *X*-H and *Y*-H bonding states and contribute more to the HOMO state. As a result of this effect, it may be difficult to design a rigid covalent framework that has strong electron-phonon contributions coming from hydrogen and contains bonds other than *X*-H.

D. Boron and carbon clusters

A more diverse class of molecular fragments arises when one considers bonding that is not reducible to pairs of atoms. Of the second-row elements, such complex bonding occurs most often in boron and carbon. In boron, this bonding leads to clusters composed of multicenter bonding such B-H-B bridging bonds and B-B-B triangular units. In carbon, delocalized electrons arise from the phenomenon of aromaticity, which happens in small molecules such as aromatic rings and can stabilize larger molecules such as fullerenes. The electron-phonon coupling strengths of a sampling of these units are calculated in Fig. 4. The diborane molecule B_2H_6 contains perhaps the simplest case of a B-H-B bridging bond. Besides the two bridging hydrogen atoms and increased B-B separation, it is structurally similar to the B_2H_4

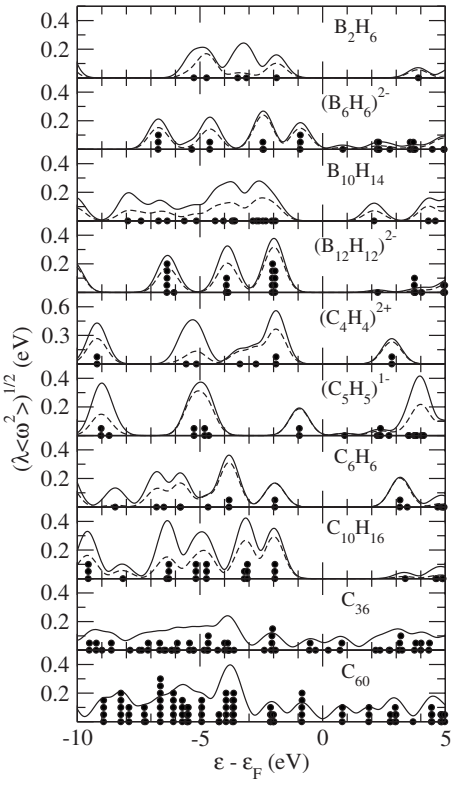

FIG. 4. Electron-phonon coupling strength in common boron and carbon clusters. Dashed curves omit the contribution from H atoms. Black circles denote energy levels and their stacking denotes degeneracy of levels.

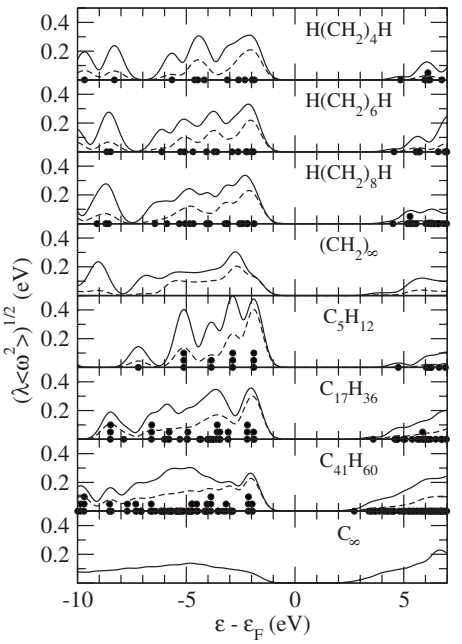

FIG. 5. Electron-phonon coupling strength in polyethylene and diamond as a function of system size. Dashed curves omit the contribution from H atoms. Black circles denote energy levels and their stacking denotes degeneracy of levels.

calculated in Fig. 3. The more stable diborane molecule has a larger HOMO-LUMO gap, but otherwise the electron-phonon coupling energy profiles are very similar between the two units, despite the addition of more hydrogen. Because of a very large degeneracy of levels in its HOMO state, the boron icosahedral unit $B_{12}H_{12}^{2-}$ has stronger electron-phonon coupling than the smaller octahedral unit $B_6H_6^{2-}$ and the less symmetric decaborane molecule $B_{10}H_{14}$. Within the small aromatic carbon rings, the fourfold ring $C_4H_4^{2+}$ has the largest electron-phonon coupling in its HOMO state. The C_{36} fullerene was predicted to have stronger electron-phonon coupling than C_{60} and was proposed to be a path to higher T_c fulleride superconductors.[32] As yet there are no experimental reports of superconductivity in C_{36} solids.[33] Within our calculations, C_{60} and C_{36} have approximately equal electron-phonon coupling strength after accounting for the degeneracy of the HOMO and LUMO states of C_{60}. As a point of reference between sp^2 and sp^3 bonds in carbon clusters, the adamantane molecule $C_{10}H_{16}$ is also plotted.

There are many extended boron-containing solids that contain octahedral, icosahedral, and other cages. Often these solids contain interstitial metal atoms that donate electrons to stabilize the boron cages in their natural charged configuration, usually with two additional electrons per cages. The hexaboride compounds XB_6 in particular show a wide degree of chemical flexibility in the possible choices of X. Superconductivity is observed with $T_c=7$ K in the case where $X=Y$.[34] This leads to electron doping of the stable B_6 unit, which corresponds to the LUMO state of $B_6H_6^{2-}$ that has very weak electron-phonon coupling to the boron atoms in Fig. 4. Hole doping occurs when $X=K$,[35] but superconductivity has not been observed in this material. We have performed preliminary calculations on the hexaboride framework, which show that electron-phonon coupling is only appreciable when less than 0.7 electrons are donated to each B_6 unit. In the case of an empty hexaboride framework with no donated electrons, our calculations show that there is a structural instability that opens up an insulating gap and destroys superconductivity. Instabilities resulting from a reduction in charge transfer from interstitial atoms to a boron framework have also been seen experimentally.[36]

E. Progression to extended systems

The relevance of these molecular fragment calculations to extended systems can be tested by considering a progression of materials from molecule to bulk. We consider such a progression in two examples: linear alkane chains approaching an infinite polyethylene chain and the construction of a diamond cluster by adding mth nearest-neighbor carbon atoms to a central carbon and hydrogen terminating all dangling bonds. Electron-phonon coupling strengths for these progressions are plotted in Fig. 5. With the Gaussian smearing of electronic levels blurring the van Hove singularities at the band edges in polyethylene, the alkane chains appear to very quickly approach the bulk energy profile of electron-phonon coupling. The diamond bulk result does not have any significant fine features for Gaussian smearing to obscure. The diamond clusters seem to converge quickly for valence states

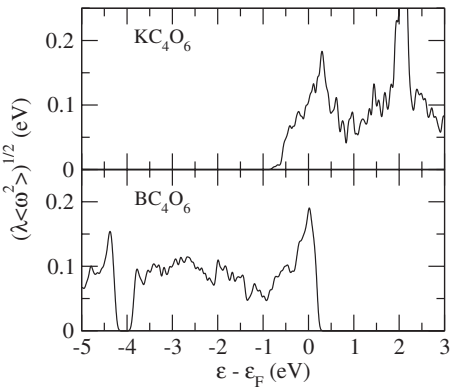

FIG. 6. Electron-phonon coupling strength in hypothetical covalent frameworks. To resolve the fine features of the electronic structure, a Gaussian smearing of 40 meV is used for these materials.

deep in energy and conduction states. An interesting feature that is slow to converge is a peak in electron-phonon coupling at the valence-band edge that gets smaller with increasing diamond cluster size.

III. HYPOTHETICAL SUPERCONDUCTORS

Using some of the molecular fragments considered in Sec. II, we now construct two examples of hypothetical superconductors using the design principles outlined in Sec. I. These materials are not designed to be easily synthesizable or to maximize T_c within some design constraint. They are just simple examples with electron-phonon coupling strength peaked near the Fermi level and wide metallic bands at the Fermi level. Both examples are constructed with a molecular unit with formula C_4O_6 in an adamantanelike structure with threefold coordinated carbon atoms and twofold coordinated oxygen atoms. The carbon atoms are not fully bonded within this fragment and are used to covalently bond fragments together.

In the first example, the C_4O_6 units are bonded to form a diamond superstructure by forming intermolecular carbon-carbon bonds. This structure is characterized by two bond lengths, C-C and C-O, which are calculated to be 1.55 and 1.42 Å. Within each interstitial site of the diamond superstructure, we place a potassium atom, which results in a crystal with the formula KC_4O_6. The potassium atoms each donate their 4*s* electron to the covalent framework, doping into its conduction band. The electron-phonon coupling strength is large at the Fermi level as shown in Fig. 6. A peak in coupling strength occurs at 0.3 eV above the Fermi level, which corresponds to the off-stoichiometric ratio of 1.5 electrons per C_4O_6 unit. Using the Γ-point approximation to the Eliashberg spectral function,[8] we estimate that $\lambda \approx 11$ at the peak in electron-phonon coupling. This large value of λ arises from the coupling with low-frequency phonon modes and anharmonic corrections are likely to harden these phonons and reduce λ. If the material is within the strong-coupling regime after corrections have been applied to λ, then its T_c may be estimated from Eq. (1) to be ~380 K.

The C_4O_6 unit can also be used to form a stable hole-doped covalent framework. This framework is constructed as a zinc-blende superstructure with C_4O_6 units on one site and boron atoms on the other site. This may be thought of as a hole-doped version of an insulating framework resulting from replacing all boron atoms with carbon. Alternatively, the structure is insulating if alkali-metal atoms are placed on half the interstitial sites of the zinc-blende framework. This structure can be interpreted as a hole-doped version of the C_5H_{12} diamondoid fragment from Fig. 5 bonded by oxygen ligands and may benefit from the large electron-phonon coupling of the HOMO state of that system. In this structure, our calculations show that boron remains stable in its tetrahedral coordination. This structure is characterized by two bond lengths, B-C and C-O, which are calculated to be 1.68 and 1.43 Å. The electron-phonon coupling peaks at the Fermi level of BC_4O_6, as shown in Fig. 6. From the Γ-point approximation to the Eliashberg spectral function, we estimate that $\lambda \approx 70$ because of very low frequency but still stable phonons. Anharmonic corrections to these soft phonons should significantly reduce the value of λ. The resulting strong-coupling T_c estimate for BC_4O_6 is ~380 K, which is essentially the same value as is estimated for KC_4O_6. This demonstrates that both electron and hole doping of a covalent framework can lead to large T_c values.

IV. CONCLUSIONS

After studying the electron-phonon coupling strength available in various molecular fragments in Sec. II, we can conclude that superconductivity at high temperatures may originate from many different molecular building blocks. Strong electron-phonon coupling to valence states is a universal feature of molecules containing covalent bonds between second-row elements. A major difficulty in designing a superconductor from covalent fragments is in creating a metallic state with strong electron-phonon coupling strength specifically at the Fermi level. As seen from Sec. III, such a design goal can be achieved given sufficient freedom in the placement of atoms. Both constructed examples are open frameworks that are able to host dopant atoms and are dopable through a process of intercalation or deintercalation. Such open frameworks also lead to electronic bands with narrow bandwidths that produce large densities of states which are beneficial for superconductivity. However, open frameworks and narrow electronic bandwidths may lead to structural and electronic instabilities that remain as important constraints on the design of such materials.

We have provided two specific examples of superconducting covalent frameworks, with transition temperatures estimated to be up to 380 K according to Eliashberg theory. If these specific materials are to be experimentally pursued, a likely precursor is the synthesis of the adamantanelike $C_4O_6X_4$ molecule, where *X* are ligands bonded to the carbon atoms. Further theoretical study of the stability of the superconducting state in these materials is also warranted.

The above estimates are intended to be suggestive of possible paths to high T_c electron-phonon superconductors. While studies of this kind do not provide a rigorous bound on T_c, it may be worthwhile to pursue the theoretical construction of hypothetical phonon-mediated superconductors with increasingly large T_c. The highest T_c material imaginable might be a practical substitute for finding the highest T_c possible.

ACKNOWLEDGMENTS

This work was supported by National Science Foundation under Grant No. DMR07-05941 and by the Director, Office of Science, Office of Basic Energy Sciences, Division of Materials Sciences and Engineering Division, U.S. Department of Energy under Contract No. DE-AC02-05CH11231.

*jmoussa@civet.berkeley.edu

[1] J. Nagamatsu, N. Nakagawa, T. Muranaka, Y. Zenitani, and J. Akimitsu, Nature (London) **410**, 63 (2001).
[2] O. Gunnarsson, Rev. Mod. Phys. **69**, 575 (1997).
[3] A. Y. Ganin, Y. Takabayashi, Y. Z. Khimyak, S. Margadonna, A. Tamai, M. J. Rosseinsky, and K. Prassides, Nat. Mater. **7**, 367 (2008).
[4] Y. Takano, T. Takenouchi, S. Ishii, S. Ueda, T. Okutsu, I. Sakaguchi, H. Umezawa, H. Kawarada, and M. Tachiki, Diamond Relat. Mater. **16**, 911 (2007).
[5] M. Calandra, N. Vast, and F. Mauri, Phys. Rev. B **69**, 224505 (2004).
[6] F. Zipoli, M. Bernasconi, and G. Benedek, Phys. Rev. B **74**, 205408 (2006).
[7] F. J. Ribeiro and M. L. Cohen, Phys. Rev. B **69**, 212507 (2004).
[8] J. E. Moussa and M. L. Cohen, Phys. Rev. B **77**, 064518 (2008).
[9] W. Grochala, J. Mol. Model. **11**, 323 (2005).
[10] A. Devos and M. Lannoo, Phys. Rev. B **58**, 8236 (1998).
[11] P. B. Allen and R. C. Dynes, Phys. Rev. B **12**, 905 (1975).
[12] J. J. Hopfield, Phys. Rev. **186**, 443 (1969).
[13] P. K. Lam and M. L. Cohen, Phys. Lett. **97A**, 114 (1983). Note that there is a typo in Eq. (6); the exponent of the electron density is supposed to be 1.2.
[14] P. K. Lam, M. M. Dacorogna, and M. L. Cohen, Phys. Rev. B **34**, 5065 (1986).
[15] E. Prodan and W. Kohn, Proc. Natl. Acad. Sci. U.S.A. **102**, 11635 (2005).
[16] H. Rosner, A. Kitaigorodsky, and W. E. Pickett, Phys. Rev. Lett. **88**, 127001 (2002).
[17] H. Li, M. Eddaoudi, M. O'Keeffe, and O. M. Yaghi, Nature (London) **402**, 276 (1999).
[18] J. Kouvetakis, R. B. Kaner, M. L. Sattler, and N. Bartlett, J. Chem. Soc., Chem. Commun. **24**, 1758 (1986).
[19] P. B. Allen and B. Mitrović, Solid State Phys. **37**, 2 (1982).
[20] A. B. Migdal, Sov. Phys. JETP **7**, 996 (1958).
[21] N. N. Bogolubov, V. V. Tolmachev, and D. V. Shirkov, *New Method in the Theory of Superconductivity* (Academy of the Sciences of the U.S.S.R., Moscow, 1958).
[22] M. Capone and S. Ciuchi, Phys. Rev. Lett. **91**, 186405 (2003).
[23] J. E. Han, O. Gunnarsson, and V. H. Crespi, Phys. Rev. Lett. **90**, 167006 (2003).
[24] G. Kresse and J. Furthmüller, Phys. Rev. B **54**, 11169 (1996).
[25] N. W. Ashcroft, Phys. Rev. Lett. **21**, 1748 (1968).
[26] K. Shimizu, K. Suhara, M. Ikumo, M. I. Eremets, and K. Amaya, Nature (London) **393**, 767 (1998).
[27] K. Shimizu, H. Ishikawa, D. Takao, T. Yagi, and K. Amaya, Nature (London) **419**, 597 (2002).
[28] T. Yabuuchi, T. Matsuoka, Y. Nakamoto, and K. Shimizu, J. Phys. Soc. Jpn. **75**, 083703 (2006).
[29] N. W. Ashcroft, Phys. Rev. Lett. **92**, 187002 (2004).
[30] M. I. Eremets, I. A. Trojan, S. A. Medvedev, J. S. Tse, and Y. Yao, Science **319**, 1506 (2008).
[31] J. Feng, W. Grochala, T. Jaron, R. Hoffmann, A. Bergara, and N. W. Ashcroft, Phys. Rev. Lett. **96**, 017006 (2006).
[32] M. Côté, J. C. Grossman, M. L. Cohen, and S. G. Louie, Phys. Rev. Lett. **81**, 697 (1998).
[33] C. Piskoti, J. Yarger, and A. Zettl, Nature (London) **393**, 771 (1998).
[34] B. T. Matthias, T. H. Geballe, K. Andres, E. Corenzwit, G. W. Hull, and J. P. Maita, Science **159**, 530 (1968).
[35] A. Ammar, M. Ménétrier, A. Villesuzanne, S. Matar, B. Chevalier, J. Etourneau, G. Villeneuve, J. Rodríguez-Carvajal, H.-J. Koo, A. I. Smirnov, and M.-H. Whangbo, Inorg. Chem. **43**, 4974 (2004).
[36] G. Mair, R. Nesper, and H. G. von Schnering, J. Solid State Chem. **75**, 30 (1988).